

## Electronic Supplementary Information

Integrated high-sulfur-loading polysulfide/carbon cathode in lean-electrolyte cell toward  
high-energy-density lithium–sulfur cells with stable cyclability

Yun-Chen Wu<sup>a</sup> and Sheng-Heng Chung<sup>\*ab</sup>

<sup>a</sup> Department of Materials Science and Engineering, National Cheng Kung University, No. 1, University Road, Tainan City, 70101

<sup>b</sup> Hierarchical Green-Energy Materials Research Center, National Cheng Kung University, No. 1, University Road, Tainan City, 70101

\*Sheng-Heng Chung: [SHChung@gs.ncku.edu.tw](mailto:SHChung@gs.ncku.edu.tw)

## Supporting Figures

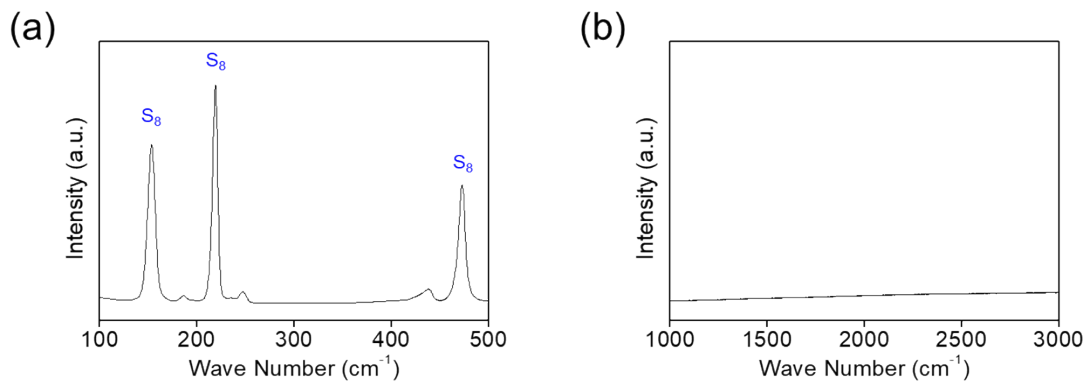


**Fig. S1.** Configuration characteristics. Raman spectra of the inner active-material core of uncycled core–shell polysulfide/carbon cathode: (a) sulfur and (b) carbon.

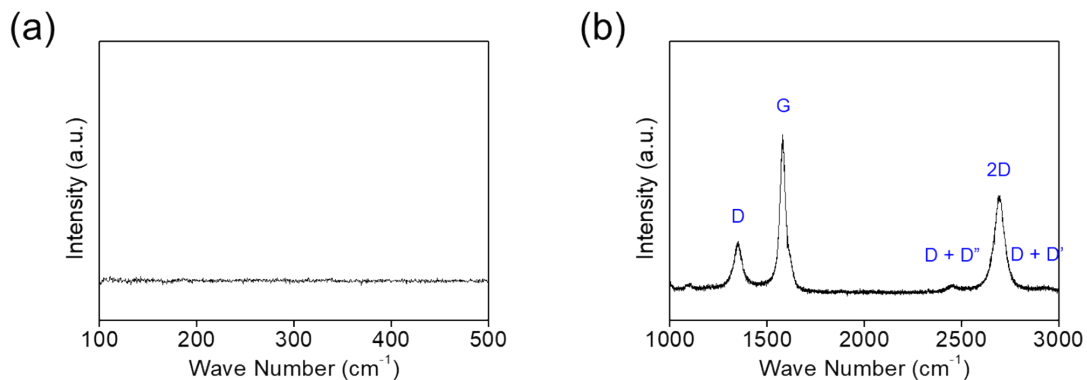


**Fig. S2.** Configuration characteristics. Raman spectra of the outer carbon shell of uncycled core–shell polysulfide/carbon cathode: (a) sulfur and (b) carbon.

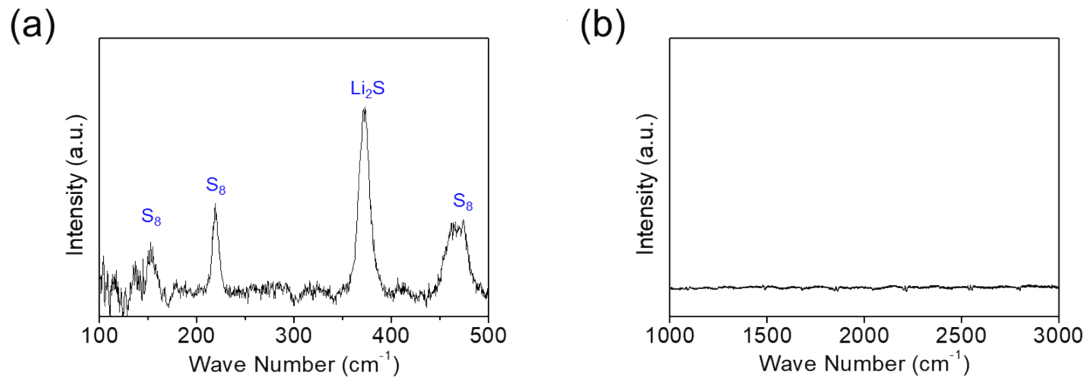


**Fig. S3.** Configuration characteristics. Raman spectra of the inner active-material core of cycled core–shell polysulfide/carbon cathode: (a) sulfur and (b) carbon.

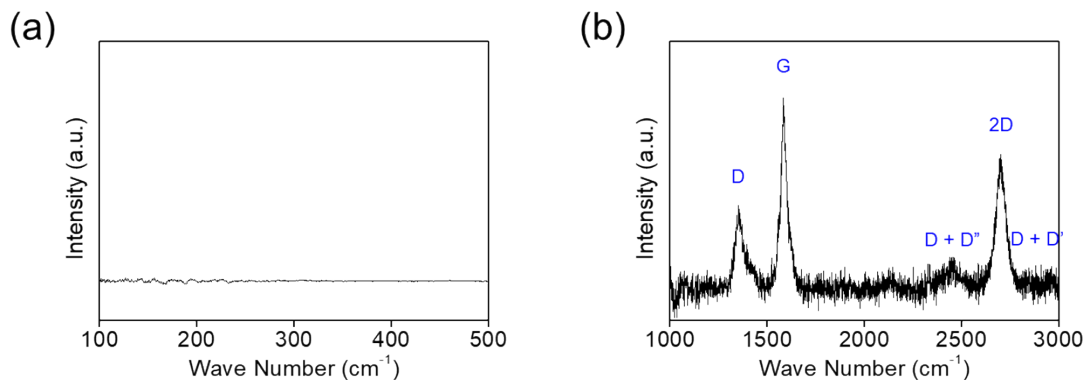


**Fig. S4.** Configuration characteristics. Raman spectra of the outer carbon shell of cycled core–shell polysulfide/carbon cathode: (a) sulfur and (b) carbon.

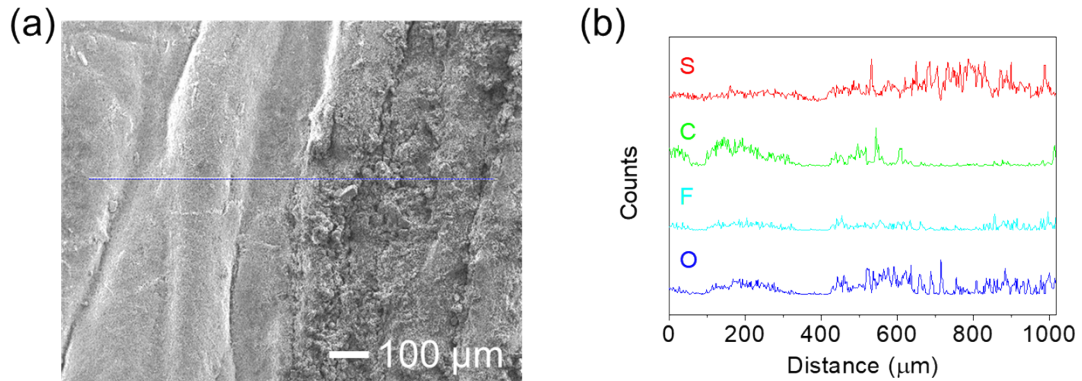


**Fig. S5.** Configuration characteristics. Line-scanning results of the core–shell interface of the cycled polysulfide/carbon cathode.

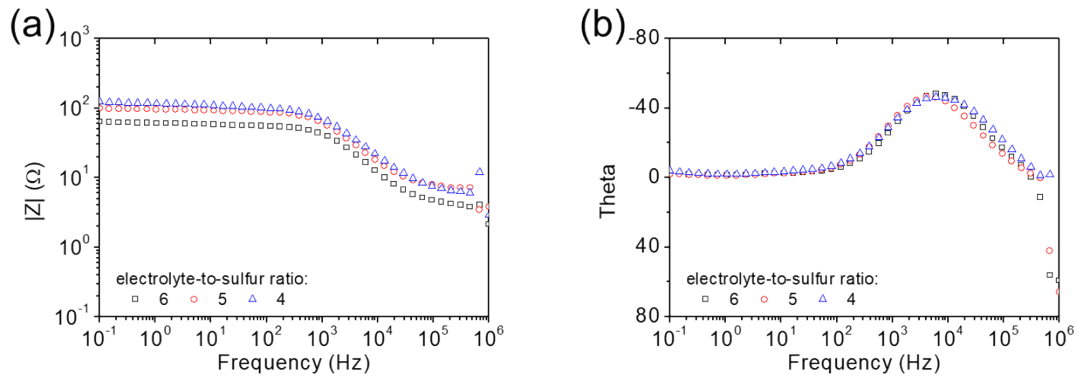


**Fig. S6.** Electrochemical characteristics. Bode plots of the uncycled high-loading core–shell polysulfide/carbon cathode in lean-electrolyte cells with electrolyte-to-sulfur ratios of 6, 5, and 4  $\mu\text{L mg}^{-1}$ .

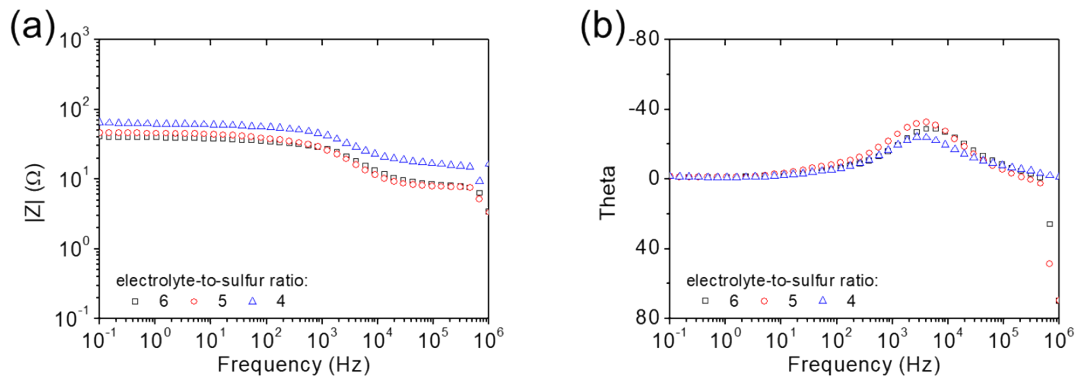


**Fig. S7.** Electrochemical characteristics. Bode plots of the cycled high-loading core–shell polysulfide/carbon cathode in lean-electrolyte cells with electrolyte-to-sulfur ratios of 6, 5, and 4  $\mu\text{L mg}^{-1}$ .

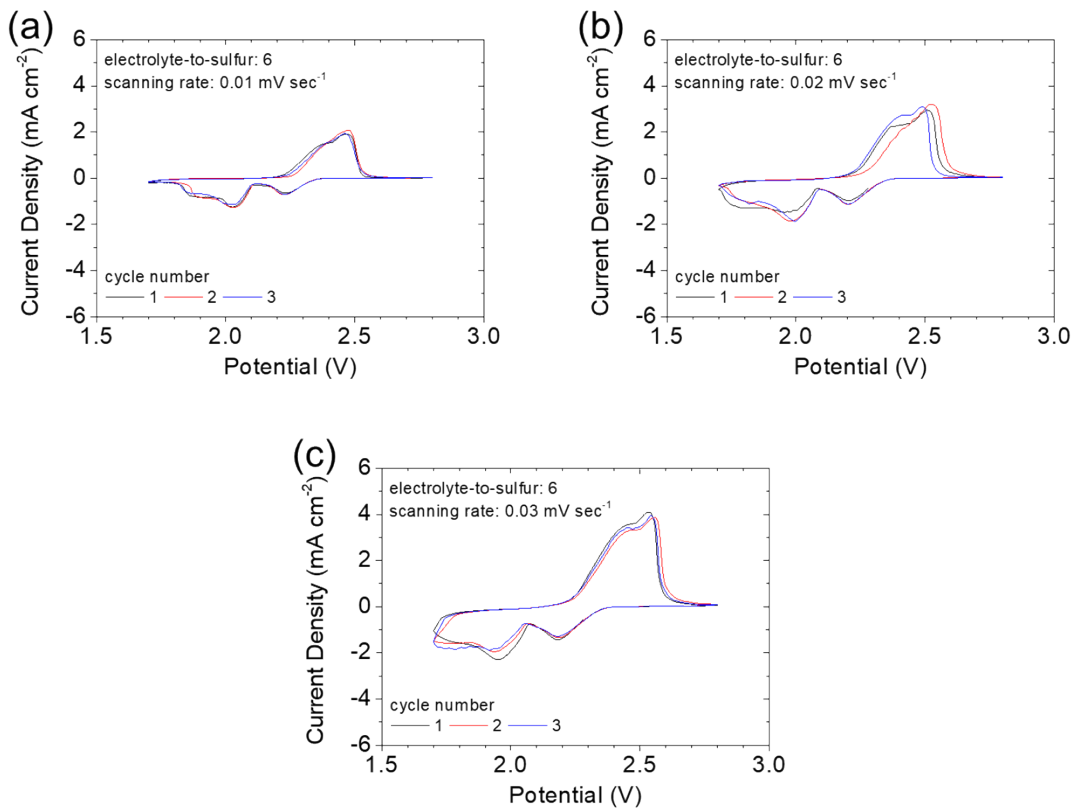


**Fig. S8.** Electrochemical characteristics. Cyclic voltammograms of the high-loading core–shell polysulfide/carbon cathode in a lean-electrolyte cell with an electrolyte-to-sulfur ratio of  $6 \mu\text{L mg}^{-1}$  at potential sweeping rates of (a)  $0.01$ , (b)  $0.02$ , and (c)  $0.03 \text{ mV s}^{-1}$ .

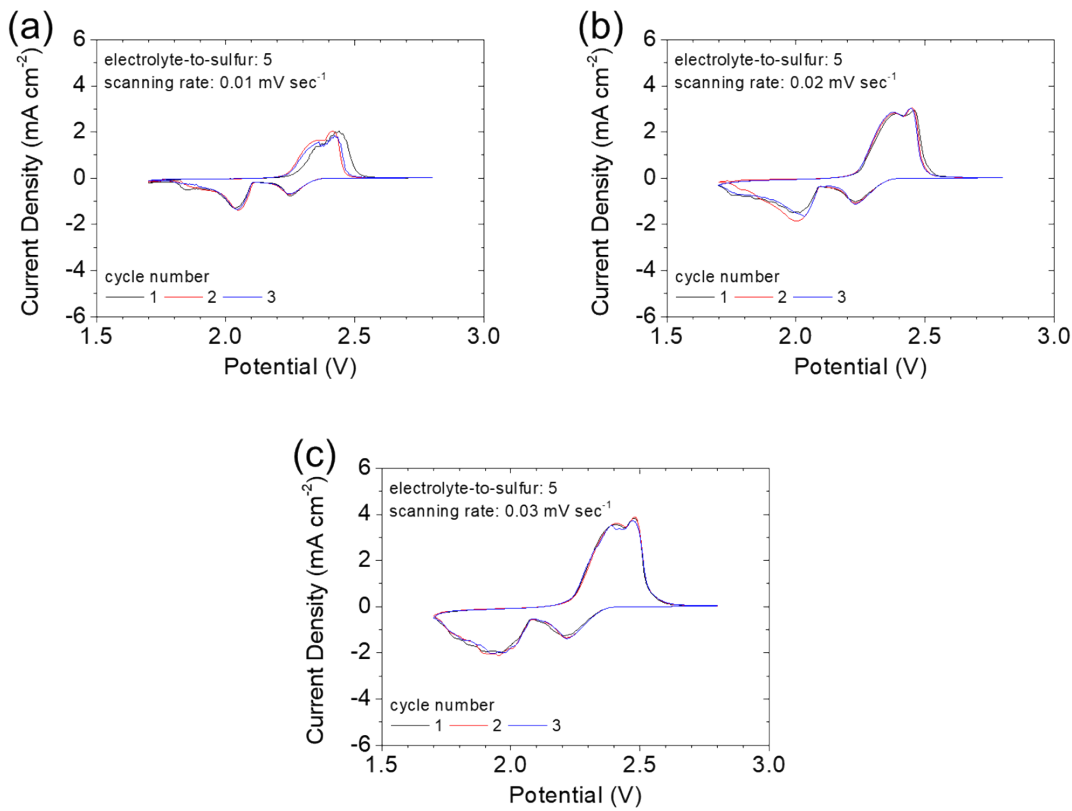


**Fig. S9.** Electrochemical characteristics. Cyclic voltammograms of the high-loading core–shell polysulfide/carbon cathode in a lean-electrolyte cell with an electrolyte-to-sulfur ratio of  $5 \mu\text{L mg}^{-1}$  at potential sweeping rates of (a)  $0.01$ , (b)  $0.02$ , and (c)  $0.03 \text{ mV s}^{-1}$ .

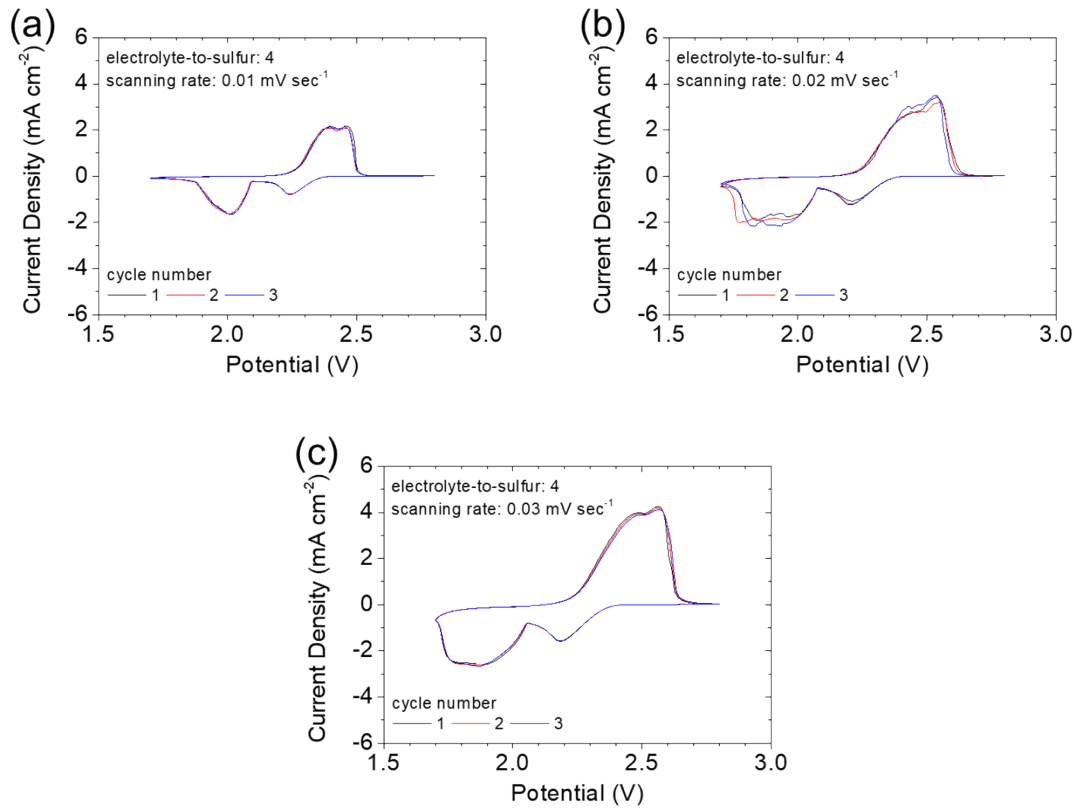


**Fig. S10.** Electrochemical characteristics. Cyclic voltammograms of the high-loading core–shell polysulfide/carbon cathode in a lean-electrolyte cell with an electrolyte-to-sulfur ratio of  $4 \mu\text{L mg}^{-1}$  at potential sweeping rates of (a)  $0.01$ , (b)  $0.02$ , and (c)  $0.03 \text{ mV s}^{-1}$ .

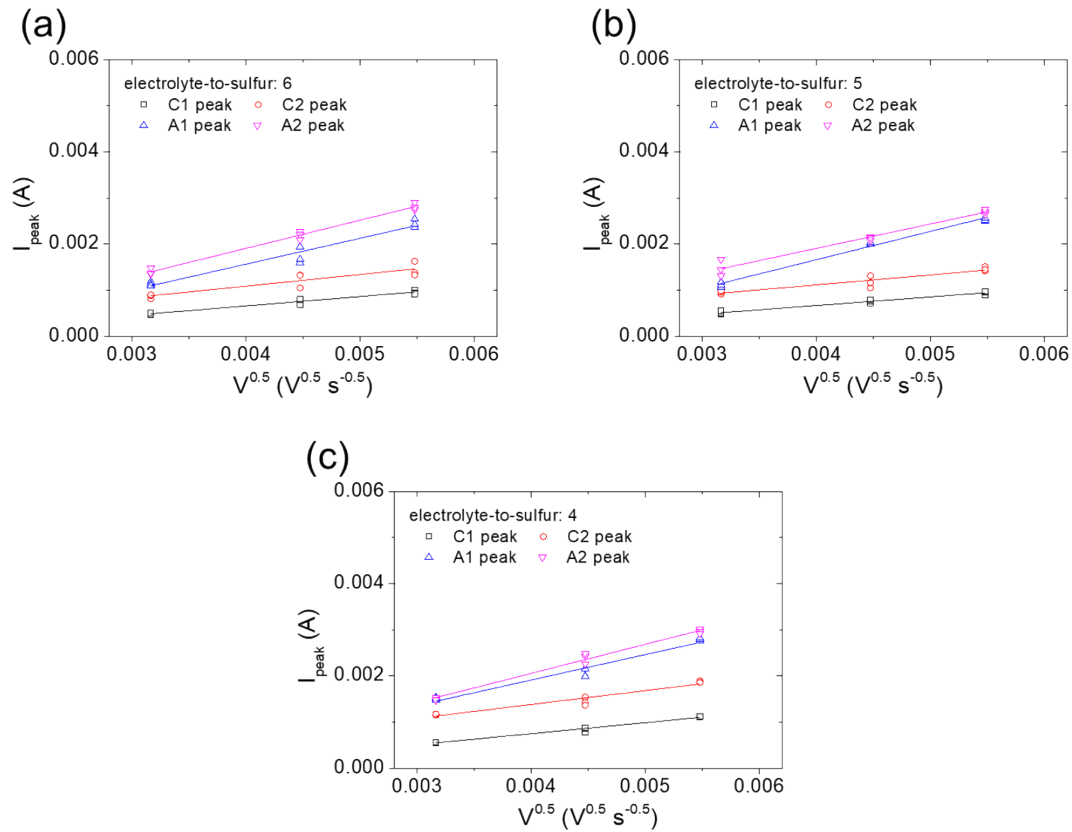


**Fig. S11.** Electrochemical characteristics. Lithium-ion diffusion coefficient of the high-loading core–shell polysulfide/carbon cathode in lean-electrolyte cells with electrolyte-to-sulfur ratios of (a) 6, (b) 5, and (c) 4  $\mu\text{L mg}^{-1}$ .

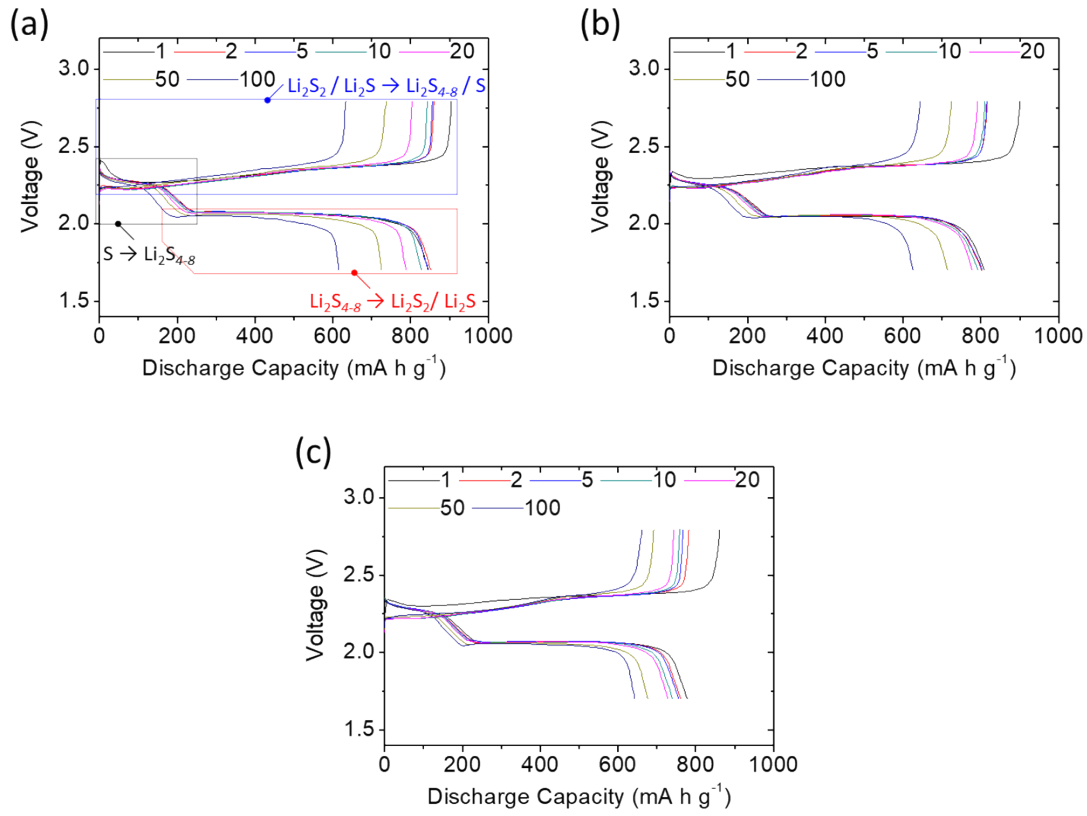


**Fig. S12.** Cell electrochemistry. Discharge/charge voltage profiles of the high-loading core–shell polysulfide/carbon cathode in a lean-electrolyte cell with an electrolyte-to-sulfur ratio of  $6 \mu\text{L mg}^{-1}$  at cycling rates of (a)  $0.10\text{C}$ , (b)  $0.15\text{C}$ , and (c)  $0.20\text{C}$ .

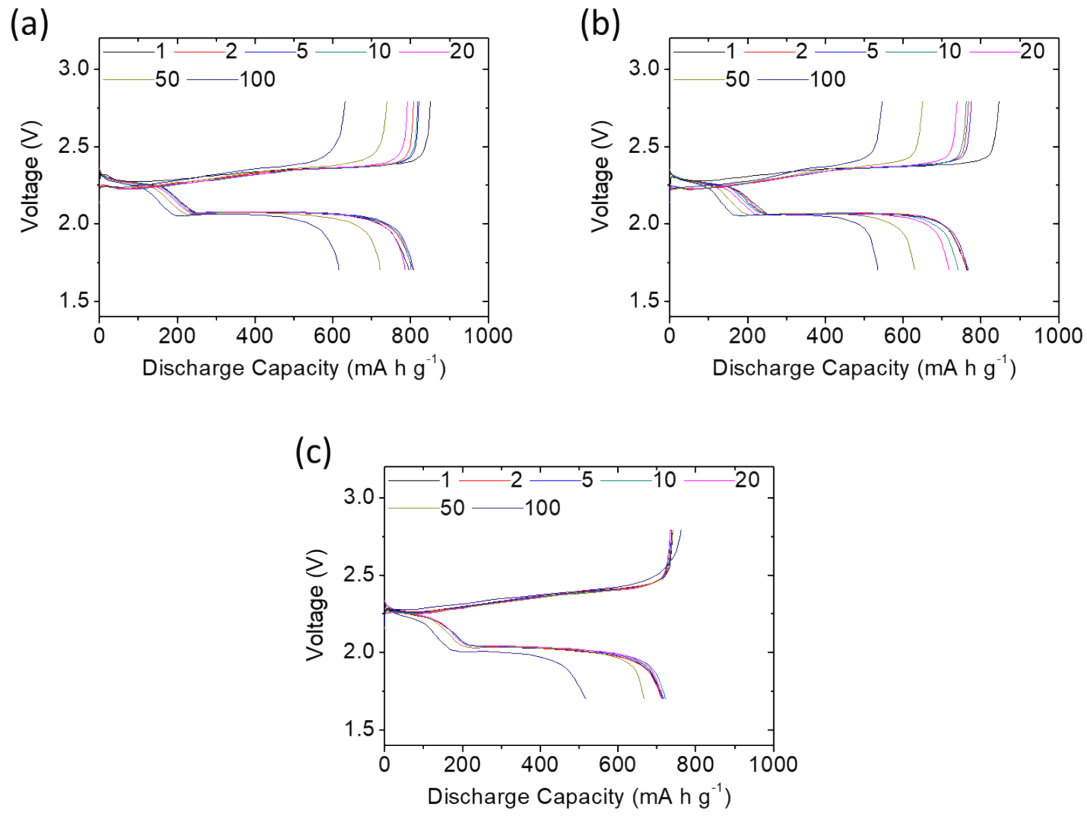


**Fig. S13.** Cell electrochemistry. Discharge/charge voltage profiles of the high-loading core–shell polysulfide/carbon cathode in a lean-electrolyte cell with an electrolyte-to-sulfur ratio of  $5 \mu\text{L mg}^{-1}$  at cycling rates of (a) 0.10C, (b) 0.15C, and (c) 0.20C.

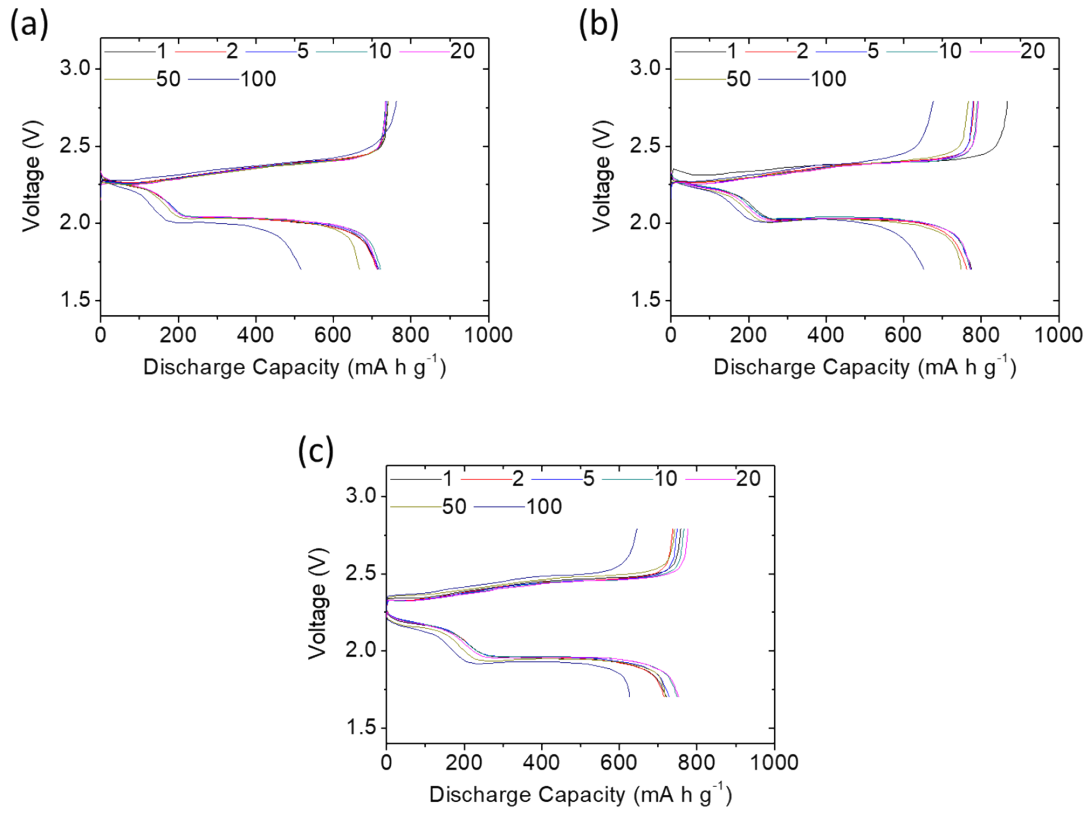


**Fig. S14.** Cell electrochemistry. Discharge/charge voltage profiles of the high-loading core–shell polysulfide/carbon cathode in a lean-electrolyte cell with an electrolyte-to-sulfur ratio of  $4 \mu\text{L mg}^{-1}$  at cycling rates of (a)  $0.10\text{C}$ , (b)  $0.15\text{C}$ , and (c)  $0.20\text{C}$ .

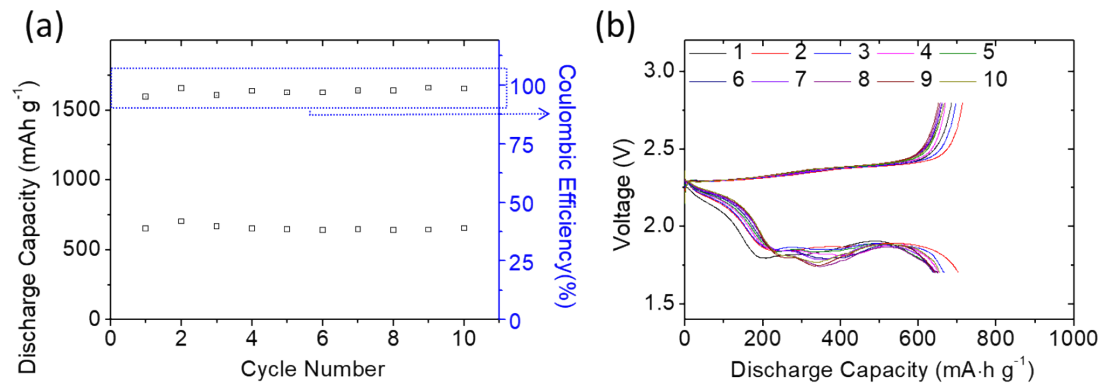


**Fig. S15.** Cell electrochemistry. (a) Cyclability and (b) discharge/charge voltage profiles of the high-loading core–shell polysulfide/carbon cathode in a lean-electrolyte cell with an electrolyte-to-sulfur ratio of  $3 \mu\text{L mg}^{-1}$  at a cycling rate of 0.10C.

## Supporting Tables

**Table S1.** Material characteristics. Specific surface area and porosity analysis of the carbon shell.

average pore size	total pore volume	specific surface area	external surface area (t-plot)
20.38 nm	0.42 cm <sup>3</sup> g <sup>-1</sup>	81.66 m <sup>2</sup> g <sup>-1</sup>	81.66 m <sup>2</sup> g <sup>-1</sup>
micropore area (t-plot)	micropore volume (t-plot)	micropore volume (DA)	micropore volume (DR)
0.0 cm <sup>3</sup> g <sup>-1</sup>	0.0 cm <sup>3</sup> g <sup>-1</sup>	0.02 cm <sup>3</sup> g <sup>-1</sup>	0.02 cm <sup>3</sup> g <sup>-1</sup>

**Table S2.** Electrochemical characteristics. Lithium-ion diffusion coefficient of the high-loading core–shell polysulfide/carbon cathode in lean-electrolyte cells with electrolyte-to-sulfur ratios of 6, 5, and 4  $\mu\text{L mg}^{-1}$ .

Electrolyte-to-sulfur ratio ( $\mu\text{L mg}^{-1}$ )	$D_{\text{Li}^+}$ of peak C1 ( $\text{cm}^2 \text{s}^{-1}$ )	$D_{\text{Li}^+}$ of peak C2 ( $\text{cm}^2 \text{s}^{-1}$ )	$D_{\text{Li}^+}$ of peak A1 ( $\text{cm}^2 \text{s}^{-1}$ )	$D_{\text{Li}^+}$ of peak A2 ( $\text{cm}^2 \text{s}^{-1}$ )
6	$4.1640 \times 10^{-8}$	$6.4326 \times 10^{-8}$	$3.1732 \times 10^{-7}$	$3.7546 \times 10^{-7}$
5	$3.4783 \times 10^{-8}$	$4.6797 \times 10^{-8}$	$3.7929 \times 10^{-7}$	$2.8188 \times 10^{-7}$
4	$5.7549 \times 10^{-8}$	$9.1525 \times 10^{-8}$	$3.0557 \times 10^{-7}$	$3.9976 \times 10^{-7}$

**Table S3.** Cell electrochemistry. Reference analysis of lean-electrolyte lithium–sulfur cells in terms of the cycling capability of the high-sulfur-loading cathode.

	Sulfur Content (wt%)	Sulfur Loading (mg cm <sup>-2</sup> )	Electrolyte-to-Capacity ratio (μL mA·h <sup>-1</sup> )	Cycle life
S01	68.8	30	n/a	100
S02	54.3	5.58	24.25	200
S03	66	7.1	8.87	167
S04	75	1.5	14.29	100
S05	64	5.5	17.65	200
S06	60.8	4	7.06	100
S07	62	3.9	15.04	100
S08	64	4.8	13.15	100
S09	64	2	7.88	100
S10	63	3.8	6.25	50
S11	56	1	8.07	100
S12	65.5	7.1	25.86	100
S13	78.09	4.17	20.13	100
S14	48	9.3	7.65	100
S15	56	3	5.70	30
S16	60	3	5.10	60
S17	56	1.9	15.89	100
S18	56	7	12.27	100
S19	60.3	10.7	9.01	60

S20	60.4	1.2	8.32	150
S21	56	7.5	13.46	50
S22	64	6	5.51	20
S23	70	1.5	13.03	150
S24	51.6	6.4	8.68	100
S25	48.1	4.3	12.18	120
S26	60	10.73	7.75	120
S27	72	6.72	10.95	100
S28	49	1	7.21	70
S29	70	7.8	9.09	100
S30	43.7	8.57	6.17	80
This work (0.10C)	64.1	12	4.80	100
This work (0.15C)	64.1	12	5.14	100
This work (0.20C)	64.1	12	5.29	200

## Supporting References

- S01 S.-H. Chung, C.-H. Chang and A. Manthiram, *Energy Environ. Sci.*, 2016, **9**, 3188-3200.
- S02 S.-H. Chung, P. Han, C.-H. Chang and A. Manthiram, *Adv. Energy Mater.*, 2017, **7**, 1700537.
- S03 R. Ummethala, M. Fritzsche, T. Jaumann, J. Balach, S. Oswald, R. Nowak, N. Sobczak, I. Kaban, M. H. Rümmeli and L. Giebel, *Energy Storage Mater.*, 2018, **10**, 206-215.
- S04 T. Lei, W. Chen, W. Lv, J. Huang, J. Zhu, J. Chu, C. Yan, C. Wu, Y. Yan and W. He, *Joule*, 2018, **2**, 2091-2104.
- S05 G. Li, W. Lei, D. Luo, Y. P. Deng, D. Wang and Z. Chen, *Adv. Energy Mater.*, 2018, **8**, 1702381.
- S06 Y. Yang, Y. Zhong, Q. Shi, Z. Wang, K. Sun and H. Wang, *Angew. Chem.*, 2018, **130**, 15775-15778.
- S07 Y.-Z. Zhang, Z. Zhang, S. Liu, G.-R. Li and X.-P. Gao, *ACS Appl. Mater. Interfaces*, 2018, **10**, 8749-8757.
- S08 Y. Qiu, X. Wu, M. Wang, L. Fan, D. Tian, B. Guan, D. Tang and N. Zhang, *ChemElectroChem*, 2019, **6**, 5698-5704.
- S09 J. S. Yeon, S. Yun, J. M. Park and H. S. Park, *ACS Nano*, 2019, **13**, 5163-5171.
- S10 M. Chen, C. Huang, Y. Li, S. Jiang, P. Zeng, G. Chen, H. Shu, H. Liu, Z. Li and X. Wang, *J. Mater. Chem. A*, 2019, **7**, 10293-10302.
- S11 Y.-W. Xu, B.-H. Zhang, G.-R. Li, S. Liu and X.-P. Gao, *ACS Appl. Energy Mater.*, 2019, **3**, 487-494.

- S12 N. Diez, G. A. Ferrero, M. Sevilla and A. B. Fuertes, *Sustainable Energy Fuels*, 2019, **3**, 3498-3509.
- S13 Z. Wang, J. Shen, J. Liu, X. Xu, Z. Liu, R. Hu, L. Yang, Y. Feng, J. Liu and Z. Shi, *Adv. Mater.*, 2019, **31**, 1902228.
- S14 Q. Pang, C. Y. Kwok, D. Kundu, X. Liang and L. F. Nazar, *Joule*, 2019, **3**, 136-148.
- S15 J. Qian, F. Wang, Y. Li, S. Wang, Y. Zhao, W. Li, Y. Xing, L. Deng, Q. Sun and L. Li, *Adv. Funct. Mater.*, 2020, **30**, 2000742.
- S16 Y. Zhang, Y. Lin, L. He, V. Murugesan, G. Pawar, B. M. Sivakumar, H. Ding, D. Ding, B. Liaw and E. J. Dufek, *ACS Appl. Energy Mater.*, 2020, **3**, 4173-4179.
- S17 W. Liang, Y. Tang, L. Liu, C. Zhu and R. Sheng, *Inorg. Chem.*, 2020, **59**, 8481-8486.
- S18 Q. Cheng, Z. Yin, S. Pan, G. Zhang, Z. Pan, X. Yu, Y. Fang, H. Rao and X. Zhong, *ACS Appl. Mater. Interfaces*, 2020, **12**, 43844-43853.
- S19 H. Yi, Y. Yang, T. Lan, T. Zhang, S. Xiang, T. Tang, H. Zeng, C. Wang, Y. Cao and Y. Deng, *ACS Appl. Mater. Interfaces*, 2020, **12**, 29316-29323.
- S20 L. Bao, J. Yao, S. Zhao, Y. Lu, Y. Su, L. Chen, C. Zhao and F. Wu, *ACS Sustainable Chem. Eng.*, 2020, **8**, 5648-5661.
- S21 D. Wang, Q. Cao, L. Li, B. Jing, Z. Yang, X. Wang, T. Huang, L. Liang, P. Zeng and J. Li, *ACS Appl. Mater. Interfaces*, 2021, **13**, 16374-16383.
- S22 Y. Zhao, J. Zhang and J. Guo, *ACS Appl. Mater. Interfaces*, 2021, **13**, 31749-31755.
- S23 Y. Li, M. Chen, H. Liu, P. Zeng, D. Zhang, H. Yu, X. Zhou, C. Guo, Z. Luo and Y. Wang, *Chem. Eng. J.*, 2021, **425**, 131640.
- S24 J. He, A. Bhargav and A. Manthiram, *ACS Nano*, 2021, **15**, 8583-8591.

- S25 H. Li, X. Wen, F. Shao, C. Zhou, Y. Zhang, N. Hu and H. Wei, *Chem. Eng. J.*, 2021, **412**, 128562.
- S26 Y. Li, W. Wang, B. Zhang, L. Fu, M. Wan, G. Li, Z. Cai, S. Tu, X. Duan and Z. W. Seh, *Nano Lett.*, 2021, **21**, 6656-6663.
- S27 Z. Tong, L. Huang, J. Guo, Y. Gao, H. Zhang, Q. Jia, D. Luo, W. Lei and S. Zhang, *Carbon*, 2022, **187**, 451-461.
- S28 X. Fan, Y. Liu, J. Tan, S. Yang, X. Zhang, B. Liu, H. Cheng, Z. Sun and F. Li, *J. Mater. Chem. A*, 2022, **10**, 7653-7659.
- S29 S. C. Jo, J. W. Hong, I. H. Choi, M. J. Kim, B. G. Kim, Y. J. Lee, H. Y. Choi, D. Kim, T. Kim and K. J. Baeg, *Small*, 2022, **18**, 2200326.
- S30 J. Wang, J. Liu, Q. Ma, X. Chen, S. Sun, H. Xu, L. Zhu, Z. Wang, J. Feng and W. Yan, *J. Alloys Compd.*, 2022, **899**, 163298.